Comparison of Solar-Thermal and Solar-Electrical-Thermal Propulsion Methods

HANS D. LINHARDT*
Aeronutronic Division, Ford Motor Company, Newport Beach, Calif.

Solar propulsion concepts recently have received increased interest, based on the intriguing simplicity of proposed designs and the availability of the free solar energy. The direct solar propulsion method has been studied in detail, whereas the indirect method has not been investigated in this country. Based on experience in direct solar propulsion systems and solar power-conversion methods, a preliminary analysis is presented in the following, which demonstrates the advantages of either system.

THE performance of solar-thermal (direct) and solar-electric-thermal (indirect) propulsion systems is analyzed and compared on the basis of payload and transfer time when applied to satellite transfer missions from 400-mile initial orbit to any high altitude earth orbit, including escape. Consistent with present booster capabilities, initial low-orbit masses ranging from 200 to 20,000 lb are considered for the performance calculations. Hydrogen is used as propellant for both thermal jets; the performance is presented as a function of the frozen flow efficiency. Based on present technology of lightweight solar collectors, the direct system appears to be limited to 900 sec specific impulse, whereas the indirect system has a potential of about 2000 sec specific impulse with arc jets and about 3000 sec with arc-jet-MHD accelerators. The optimum specific impulse of the indirect system depends on the mission parameters and the frozen flow efficiency. For fast missions (thrust to initial weight $T_0/m_0 = 10^{-3}$) and for propulsion purposes only, the direct system is superior, whereas the indirect system outperforms the direct propulsion system for most missions that require large electrical power supplies as payload. For missions specifying some electrical power and short to medium transfer times ($T_0/m_0 = 10^{-3} - 10^{-4}$), a direct propulsion scheme with a thermally integrated electrical powerplant (hybrid system) appears very promising.

Performance Parameters

Generally, the performance of a propulsion system is determined by the payload ratio (m_p/m_0), which can be delivered in the specified transfer time to the specified earth orbit or target. m_p denotes the mass of the payload and m_0 is the initial mass of the satellite or space vehicle. For the present investigation m_0 is defined as the initial mass, boosted by a chemical rocket in a low altitude 400-mile earth orbit. Considering low-thrust missions from 400-mile initial orbit to any desired earth orbit up to escape, the payload ratio (m_p/m_0) is given by the following relation:

$$\left(\frac{m_p}{m_0}\right) = \frac{1}{1 + [\gamma/(m_w/m_0)]} - \frac{m_w}{m_0} - \frac{m_s}{m_0} \qquad (1)$$

where

m_p = mass of payload
m_0 = initial mass of satellite
m_w = mass of the power supply system
m_s = mass of the structure, the empty propellant tanks, residual propellants, and the propulsion system, excluding the power supply system
γ = dimensionless acceleration parameter or thrust schedule parameter

The parameter γ is defined by the following equation:

$$\gamma = \frac{1}{737.6 g_c}\left(\frac{\alpha}{2}\right)\int_0^{t_e} a^2 dt \qquad (2)$$

where

g_c = conversion constant 32.174 lb-mass ft/lb-force sec^2
α = specific weight of power supply, lb/kw
a = acceleration at time t, ft/sec^2
t = time, sec
t_e = total transfer time, sec

It should be noted that the specific powerplant weight, α, is defined herein as the specific weight per kw of kinetic energy in the thermal jet.

If the acceleration parameter γ and the powerplant ratio m_w/m_0 are independent variables, Eq. (1) indicates that there exists an optimum powerplant weight for each mission. For example, differentiation of Eq. (1) with respect to the powerplant mass ratio determines the minimum powerplant weight;

$$(m_w/m_0)_{\min} = \gamma^{1/2} - \gamma \qquad (3)$$

and hence, the maximum payload ratio as a function of the acceleration parameter γ is

$$(m_p/m_0)_{\max} = (1 - \gamma^{1/2})^2 - (m_s/m_0) \qquad (4)$$

If the values of γ, m_w/m_0, and m_s/m_0 are known for each propulsion system as a function of a given initial mass m_0 and specified mission, the advantage of either system can be evaluated by means of the payload efficiency, η_p, which is defined in this report as the ratio of the payload ratio of the indirect system to the payload ratio of the direct system

$$\eta_p = \frac{(m_p/m_0)_i}{(m_p/m_0)_0} = \frac{(m_p)_i}{(m_p)_0} \qquad (5)$$

The subscript i refers to the indirect system and the subscript 0 identifies the direct system. Evaluation of η_p for various practical missions is the objective of the present analysis.

For this purpose the following simplification and assumptions are made:

1) Constant acceleration for both systems.

2) The structural mass ratio of both systems is the same, i.e., $(m_s/m_0)_i = (m_s/m_0)_0 = k_s$.

3) The power-supply mass ratio of the indirect system $(m_w/m_0)_i$ includes heat storage necessary for continuous thrusting but does not include the weight of the electrical transmission equipment necessary for operation of an electrothermal jet.

4) The power-supply mass ratio of the direct systems $(m_w/m_0)_0$ includes only the collector weight and does not include heat storage weight.

Condition 1 is in agreement with the findings of Refs. (4) and (5), which have shown that the constant thrust schedule is near optimum for low-thrust orbit missions and little is

Presented at the IAS 31st Annual Meeting, New York, January 21–23, 1963. This paper is based upon a study sponsored by Aeronutronic, a Division of Ford Motor Company.

* Supervisor, Space Power Section, Research Laboratory.

gained with a continuous but varying thrust schedule. At this point it should be noted that if a variable thrust vector nozzle and high-temperature heat storage materials are not developed for the direct propulsion system, intermittent thrusting with coasting periods becomes necessary,[2] reducing the payload ratio.

For constant low-thrust missions the vehicle spirals outward from the low-altitude orbit at an angle of attack so low that the orbit may be considered circular and the acceleration may be approximated by the following relation:

$$a \backsimeq (T/m_0)g_c = \text{const} \tag{6}$$

T/m_0 denotes the thrust to initial mass ratio, and g_c is the gravitational constant (32.176 lb mass-ft/lb force sec^2). Equation (6) results in negligible error for sufficiently low-thrust systems ($T/m_0 \leqq 10^{-3}$) even though appreciable changes occur during the course of the mission.[1] With the forementioned assumptions the orbit equation considering only two-body effects may be written in the following simplified form:

$$\frac{dr}{dt} = \frac{2r^2}{g_0 r_0^2}\left(\frac{g_0 r_0^2}{r}\right)^{1/2} g_c \frac{T}{m_0} \tag{7}$$

where r_0 denotes the radius of the earth, r is the radius of the specified orbit, and g_0 is the terrestrial gravitational constant. Integration of Eq. (7) determines the transfer time for a satellite spiraling from radius r_1 outward to radius r_2:

$$\Delta t = \frac{r_0}{(g_0 r_0)^{1/2}(T/m_0)}\left[\left(\frac{r_0}{r_1}\right)^{1/2} - \left(\frac{r_0}{r_2}\right)^{1/2}\right] \tag{8}$$

Figure 1 presents the transfer times calculated by means of Eq. (8) as a function of the thrust to initial weight ratio and orbit missions ranging from $r_2/r_0 = 2$ to $r_2/r_0 \rightarrow \infty$ (escape). The initial orbit has been assumed to be $r_1 = 400$ miles. Figure 1 indicates that relatively fast missions are characterized by $T/m_0 = 10^{-3}$, whereas medium transfer times are identified by $T/m_0 = 10^{-4}$ and extremely slow missions result from thrust to weight ratios of $T/m_0 = 10^{-5}$. The characteristic velocity, defined by

$$V_{CH} = \int_0^{t_e} \frac{T}{m_0} g_c dt \tag{9}$$

for constant low-thrust missions is given by the following relation:

$$V_{CH} = (T/m_0)g_c \Delta t \tag{10}$$

Substituting Δt from Eq. (8) into Eq. (10) the following relation is obtained for the characteristic velocity V_{CH}:

$$V_{CH} = (g_0 r_0)^{1/2}[(r_0/r_1)^{1/2} - (r_0/r_2)^{1/2}] \tag{11}$$

Using Eqs. (6) and (10), the acceleration parameter can now be represented in the following form:

$$\gamma = (1/2\cdot 737)\alpha\, V_{CH}(T/m_0) \tag{12}$$

which will be used for the present study.

The assumption of equal structural mass ratio for the direct and indirect system is believed to be a good approximation for the comparison of two satellites having the same initial weight, m_0, and low-pressure hydrogen storage subsystems. Assumptions 3 and 4 imply that the weight of the heat storage subsystem of the direct system is equal to the weight of the electrical transmission equipment of the indirect system and hence may be included in the structural mass ratio $k_{si} = k_{s_0} = k_s$. This simplification is necessary since conclusive data are not available yet for high-temperature thermal energy storage materials and flight type electrical transmission equipment necessary for operating arc and arc-MHD accelerators. However, cursory calculations have indicated that these assumptions lead to conservative results for arc-jet acceleration, whereas for arc-jet-MHD operation somewhat optimistic payload ratios may result for the indirect system. The effect of assumptions 3 and 4 upon the result of the present study will be discussed again.

Performance of Direct System

The direct solar propulsion system consists of the following three subsystems: the collection subsystem, the hydrogen storage subsystem, and the propulsion subsystem. The purpose of the collection subsystem is to intercept solar radiation with a parabolic collector, to focus and to absorb the energy efficiently on the hydrogen heat-exchanger of the propulsion subsystem. The propulsion subsystem comprises the hydrogen heat exchanger, controls, and the thrust nozzle. The purpose of the hydrogen storage subsystem is to store and transfer the liquid hydrogen to the propulsion subsystem. The simplicity of the direct system is striking and indicates the potential of a high reliability, long duration propulsion method. The performance of the direct system depends mainly upon the efficiency of the collection subsystem. The collection efficiency is a function of the collector-absorber geometry, the collector accuracy, and the spectral properties of collector and absorber surface materials. The thermal performance of the direct propulsion system is determined by the system efficiency $\bar{\eta}_0$, which is defined as the product of the following component efficiencies:

$$\bar{\eta}_0 = (\eta_{ca}\cdot \eta_s \cdot \eta_F)_0 \tag{13}$$

η_{ca} is the collection efficiency defined as ratio of the amount of solar energy absorbed by the heat receiving unit to the amount of solar radiation intercepted by an ideal collector. η_s denotes the heat storage factor, which is a function of the average dark time t_d to light time t_e ratio of the specified mission and the insulation efficiency η_{ins} of the heat storage subsystem according to the following equation:

$$\eta_s = \frac{1}{1 + (t_d/t_e\eta_{ins})} \tag{14}$$

The frozen flow efficiency η_F is defined as the ratio of the available thermal jet power divided by the total power put into the propellant:

$$\eta_F = [\dot{w}(H_0 - H_F)/\dot{w}\, H_0] = 1 - (H_F/H_0) \tag{15}$$

where $\dot{w}$ is the weight flow of the propellant and H_F is the enthalpy frozen in dissociation, ionization, and vaporization. For equilibrium conditions η_F amounts to unity, whereas for frozen conditions η_F depends on the propellant and the propellant temperature.[7] Reference (7) has shown that hydrogen appears to be the only candidate for present high-temperature, material-limited, thermal propulsion methods, whereby the relatively low, frozen flow performance cannot be avoided. However, for $J \leqq 900$ sec, η_F amounts to about $\eta_F \geqq 0.93$, thus indicating a favorable propellant performance.

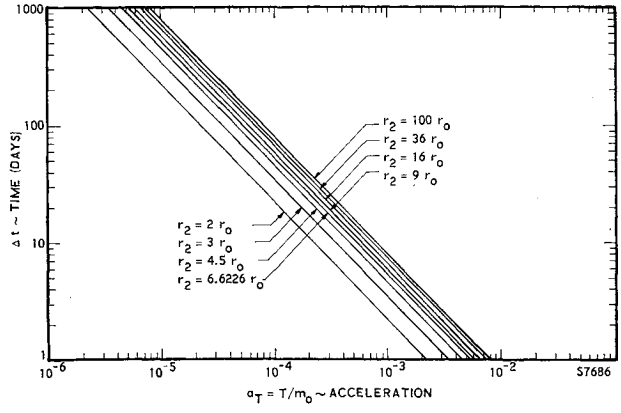

Fig. 1 Transfer time for orbit missions of low thrust propulsion systems

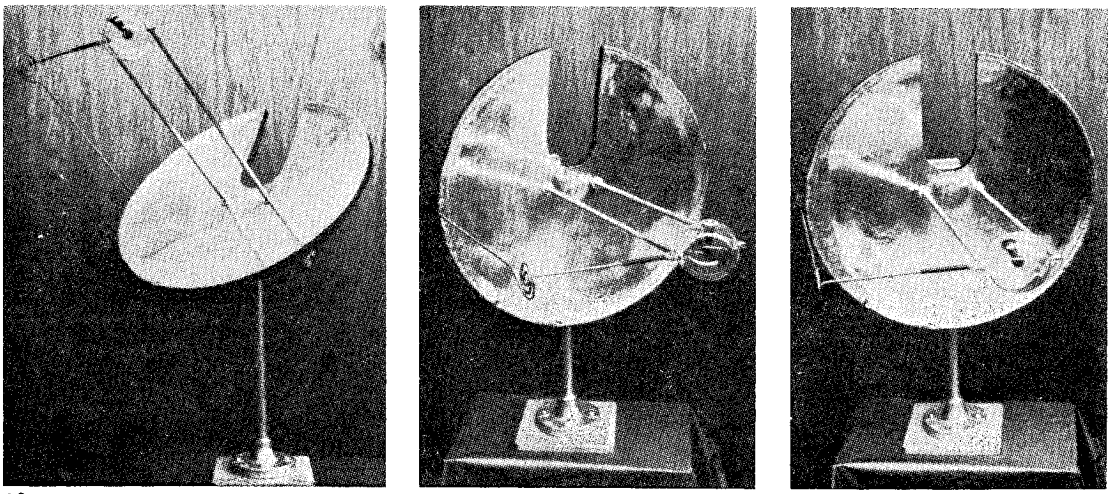

0° position 90° position 170° position

Fig. 2 Model of direct propulsion system

For analyzing a direct system without heat storage but given collector size, thrust level, and specific impulse, the system efficiency can be calculated from the following relation:

$$\bar{\eta}_0 = \frac{\text{jet power}}{\text{solar power}} = \frac{T_0 J_0/45.8}{A \cdot H/3413} \tag{16}$$

where

T = thrust, lb
J = specific impulse, sec
A = projected collector area, ft²
H = solar constant; in vicinity of earth H = 443 Btu/ft² hr

For example, the system's efficiency of the direct system proposed by Ref. 2 without heat storage capability and with a fixed thrust vector nozzle is calculated to be $\bar{\eta}_0 = 0.46$ based on Eq. (16) and the following performance parameters: collector diameter $D = 30$, ft; thrust $T = 2.2$, lb; specific impulse $J = 881$, sec. It is to be noted that Ref. 2 selected a heat receiving unit of the flat plate type, which is not particularly adaptable for integration with a reliable swivel-type nozzle. However, the performance penalty caused by a fixed thrust vector nozzle can be avoided by selection of a spherical absorber geometry[1] that allows the design of a cold, leakproof, and, therefore, reliable swivel mechanism. Figure 2 shows a model of Aeronutronic's direct propulsion system that consists of the collector and the integrated absorber, heat exchanger propulsion subsystem. The latter consists of a transparent containment sphere, the absorber-heat exchanger, and the expansion nozzle. Figure 3 presents a preliminary layout drawing of the propulsion subsystem assembly. In operation, the collector focuses the intercepted solar energy upon the absorber-heat exchanger located in the center of the containment sphere. Hydrogen enters the containment sphere through a flexible tube, is deflected, circulates around the surface, and then migrates to the center due to the pressure gradient. After picking up heat from the containment sphere wall, the hydrogen diffuses through the porous wall of the absorber-heat exchanger and is exhausted through the nozzle. The porous heat exchanger is the surface of highest temperature on which the solar energy is focused. For this purpose the diameter of the absorber sphere has to be selected closely equal to the diameter of the sun's image generated by the collector of given surface accuracy in order to achieve an efficient, high-temperature collection subsystem.

The containment sphere can be rotated in one plane through about 160° of arc (shown in a sequence of pictures in Fig. 2); by rotating the entire assembly about the focal axis, thrust is possible in all but about 11% of possible directions. Thrusting in all directions is made possible by providing a notch in the collector as shown in Fig. 2. Thus, freedom of choice of the thrust vector is achieved without the complication of a swivel nozzle. Presentation of the detailed heat transfer and performance analysis of the system just described is beyond the scope of the present paper. The thermal performance of Aeronutronic's direct propulsion system is summarized by the following parameters: collector diameter $D = 10$, ft; thrust $T = 0.25$, lb; specific impulse $J = 850$, sec. The efficiency for this system is $\bar{\eta}_0 = 0.455$. It may be concluded that the performance of present direct solar propulsion systems is characterized by the following parameters: maximum specific impulse $J \leqq 900$ sec; system's efficiency $\bar{\eta}_0 \leqq 0.46$; (excluding heat storage $\eta_s = 1$). These parameters will be used in the analysis and comparison of direct and indirect systems given below.

The payload ratio $(m_p/m_0)_0$ is now evaluated as follows. The specific powerplant weight, α_0, of the direct system is determined by the following equation:

$$\alpha_0 = [(3413\ \gamma_{c_0})/(H \cdot \bar{\eta}_0)] \tag{17}$$

where γ_{c_0} denotes the specific weight of the collector. Recent developments[3, 6] indicate that the specific weight of space collectors having a high degree of surface accuracy is approximated best by the value of $\gamma_c \geqq 0.36$ (lb/ft²). The heat storage factor η_s is estimated to be $\eta_s = 0.66$ throughout the present study. Then the efficiency of the direct system with heat storage amounts to $\bar{\eta}_0 = 0.304$. With the values of performance parameters just listed, the acceleration parameter γ_0 of the direct system is established:

$$\gamma_0 = (V_{CH}/161) \cdot (T_0/m_0) = C_1(T_0/m_0) \tag{18}$$

The powerplant mass ratio, defined by

$$(m_w/m_0)_0 = \alpha_0 \cdot (\text{kw}_{\text{jet}}/m_0) \tag{19}$$

is given by inserting the relations for kw_{jet} [Eq. (16)] and α_0 [Eq. (17)] into Eq. (19):

$$\left(\frac{m_w}{m_0}\right)_0 = \frac{3413\gamma_{c_0}}{H \cdot \bar{\eta}_0} \cdot \frac{(T_0/m_0)J_0}{45.8} = C_2 J_0 \cdot \left(\frac{T_0}{m_0}\right) \tag{20}$$

The constant C_2 is 0.198 for the assumptions made. With γ_0 and $(m_w/m_0)_0$ known, the payload ratio $(m_p/m_0)_0$ is determined as follows:

$$\left(\frac{m_p}{m_0}\right)_0 = \frac{1}{1 + (C_1)/(C_2 J_0)} - C_2 J_0 \left(\frac{T_0}{m_0}\right) \tag{21}$$

Since γ_0 and $(m_w/m_0)_0$ are not independent variables, there does not exist an optimum powerplant for each mission, but

an optimum specific impulse J_{opt}. The optimum specific impulse of the direct system is obtained by differentiation of Eq. (21), yielding the following result:

$$(J_0)_{opt} = \left(\frac{C_1}{C_2^2 T_0/m_0}\right)^{1/2} - \frac{C_1}{C_2} \tag{22}$$

Figure 4 presents the optimum specific impulse of the direct propulsion system as a function of the mission parameter r_2/r_0 and the thrust to weight ratio T_0/m_0. Figure 4 indicates that for the missions of interest $J_0 = 900$ sec approaches closely the optimum specific impulse for $T_0/m_0 = 10^{-3}$, whereas for all other thrust to weight ratios, $T_0/m_0 < 10^{-3}$ specific impulses higher than $J_0 = 900$ sec are required. Since values less than $J_0 \leqq 900$ sec are nonoptimum and the present direct system is limited to $J_0 = 900$ sec, a constant value of $J_0 = 900$ sec will be used for further calculations.

Performance of Indirect System

The indirect system consists of five major subsystems: the collection subsystem, the energy conversion subsystem, the electrical transmission and control subsystem, the hydrogen storage and transfer subsystem, and the propulsion subsystem. The collection subsystem is comprised of the solar collector and the heat receiving unit. The purpose of the solar collector is to intercept solar energy and then to focus this energy into the heat-receiving unit. The heat receiver stores part of this energy for dark-side operation and transfers heat to the power conversion subsystem as required. The power conversion subsystem converts the heat available from the heat receiving unit into useful electrical power and disposes of all waste heat associated with its modes of operation. The collection and power conversion subsystems are integrated into the solar powerplant by means of the heat transfer medium and the control subsystem.

The purpose of the control subsystem is to control the collection, the heat storage, rejection, conversion, and distribution of energy. The electrical transmission subsystem transfers the electrical energy to the propulsion subsystem in the modes required by arc jet or arc jet-MHD accelerator operation. The hydrogen storage subsystem stores and transfers the propellant to the propulsion subsystem in the amount required by the specified thrust schedule. The system efficiency $\bar{\eta}_i$ of the indirect propulsion system is defined by the following relation, which takes into account the performance of each subsystem:

$$\bar{\eta}_i = \{\eta_{ca} \cdot \eta_{pc} \eta_s [(\eta_{el} \cdot \eta_F)/\eta_R]\}_i \tag{23}$$

where

η_{ca} = collection efficiency, defined as the ratio of the useful energy absorbed in the heat receiving unit to the total solar energy intercepted by the collector

η_{pc} = power conversion efficiency, defined as the ratio of the useful electrical power output of the conversion subsystem to the energy provided by the heat receiving unit

η_{el} = electrical efficiency of transmission equipment

η_F = frozen flow efficiency

η_R = regeneration factor, defined as $\eta_R = (1 - \Delta h/H)$ where Δh is the amount of waste heat of a power conversion subsystem useful for preheating of propellant, and H is the total amount of energy required to put into the propellant for achieving desired performance

η_s = heat storage factor

The system efficiency defined by the forementioned equation depends upon collector accuracy, spectral performance of the collector, heat-receiving surface materials, specified magnitude and distribution of the temperature of the heat receiving unit, geometry of the collector and heat receiving unit, type of energy conversion method, and the power requirements of the thermal jet. Compared with the direct system, the collection subsystem of the indirect system may operate at lower temperature levels, leading to a decrease of reradiation losses and therefore to an increase of the collection efficiency. Based on recent developments of highly accurate space collector surfaces[6] identified by a standard surface accuracy value of $\sigma = 0.21$, it is possible to achieve collection efficiencies close to $\eta_{ca} = 0.88$. The energy conversion efficiency depends to a large degree upon whether the conversion method is static or dynamic and upon the specified electrical power output of the powerplant. The present state-of-the-art prefers static or direct conversion methods (photovoltaic and thermionic) for the power range $0 < \text{kw}_e < 1.5$, whereas dynamic (turbo-electric) conversion subsystems dominate the power range above 1 kw_e.[3, 8, 9]

Detailed analysis conducted by the author for solar turbo-electric powerplants, including heat storage, has shown that the specific powerplant weight of advanced solar dynamic systems can be represented by the following empirical relations:

$$(\alpha_p)_i = 181.2/(\text{kw}_e)_i^{0.37} \tag{24}$$

For the present study, Eq. (24) will be used for determination of the specific powerplant weight α_i, and the powerplant mass ratio $(m_w/m_0)_i$ of the indirect system. Combining Eqs. (24) and (13) and observing that α_i has been defined as specific powerplant weight per kw of jet power, the specific weight α_i is given by the following relation:

$$\alpha_i = 743(\eta_R/\eta_F \cdot \eta_{el})^{0.63} \cdot T_i^{-0.37} \cdot J_i^{-0.37} \tag{25}$$

Then the powerplant mass ratio $(m_w/m_0)_i$ is determined in accordance with Eq. (19).

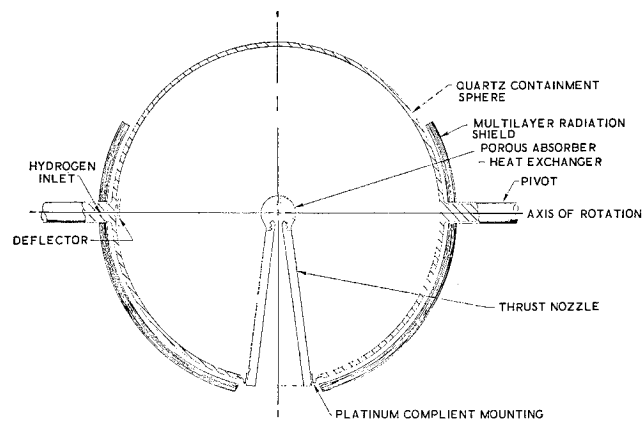

Fig. 3 Direct propulsion subsystem assembly

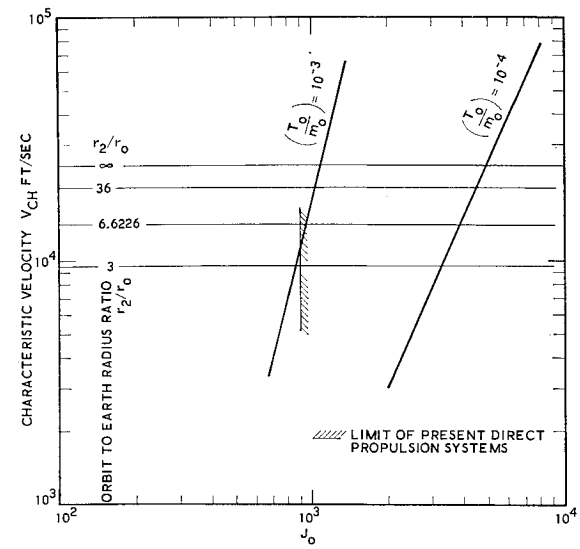

Fig. 4 Optimum specific impulse of direct propulsion system

$$\left(\frac{m_w}{m_{0i}}\right)_i = 16.3\left(\frac{\eta_R}{\eta_F\cdot\eta_{el}}\right)^{0.63} J_i^{0.63}\frac{T_i^{0.63}}{m_0} = C_3\left(\frac{\eta_R}{\eta_F\cdot\eta_{el}}\right)^{0.63} J_i^{0.63}\frac{T_i^{0.63}}{m_0} \quad (26)$$

Equation (26) indicates that the powerplant mass ratio $(m_w/m_0)_i$ is dependent upon the thrust to weight ratio (T_i/m_0), the specific impulse J_i, the thermal jet efficiency, and the magnitude of the initial mass m_0. With the abreviation,

$$\varphi_i = [\eta_R/(\eta_F\cdot\eta_{el})]_i \quad (27)$$

the acceleration parameter γ_i of the indirect system is given by the following relation:

$$\gamma_i = C_4\,\varphi_i^{0.63} J_1^{-0.37}(T_i^{0.63}/m_0) \quad (28)$$

where

$$C_4 = 0.48\cdot V_{CH}$$

$$\eta_R = 0.85 \qquad \eta_{el} = 0.90 \qquad \eta_F = f(J_i)$$

Combining Eqs. (27) and (28), the payload ratio $(m_p/m_0)_i$ is determined in accordance with Eq. (1) by the following expression:

$$\left(\frac{m_p}{m_0}\right)_i = \frac{1}{1 + (C_4)/(C_3 J_i)} - C_3\varphi_i^{0.63} J_i^{0.63}\frac{T_i^{0.63}}{m_0} \quad (29)$$

The optimum specific impulse as a function of mission ($C_4 \sim V_{CH} \sim r_2/r_0$), initial mass, m_0, and thrust to weight ratio, T_i/m_0, is determined by the following equation obtained by optimization of Eq. (29):

$$0.63\,C_4\,\varphi_i^{0.63}(T_i^{0.63}/m_0)[(C_3/C_4)J_i + 1]^2 - J_i^{0.37} = 0 \quad (30)$$

By defining the mission function F_i,

$$F_i = 0.63\,C_4\,\varphi_i^{0.63}(T_i^{0.63}/m_0) \quad (31)$$

and rearranging Eq. (30) to the following form,

$$F_i = J_i^{0.37}/[(C_3/C_4)J_i + 1]^2 \quad (32)$$

the optimum specific impulse $(J_{opt})_i$ can be determined graphically for given values of F_i. For this purpose Fig. 5 is prepared, which presents the optimum specific impulse of the indirect system as a function of the mission function F_i and the mission parameter r_2/r_0. Based on Fig. 5 the optimum specific impulse has been calculated as a function of the initial mass m_0, the thrust to weight ratio T_i/m_0, and the mission parameter r_2/r_0 as shown in Fig. 6. Figure 6 indicates that the indirect propulsion method is not competitive for short-time missions identified by the thrust to weight ratio of $T_i/m_0 = 10^{-3}$, since the optimum specific impulse is less than the specific impulse achievable by the direct system $J_0 = 900$ sec for all initial masses $200 \leqq m_0 \leqq 3.10^4$ lb. Then it is obvious that for $T_i/m_0 \geqq 10^{-3}$ the indirect system is less efficient than the direct system due to higher fuel weight and the additional weight of the power conversion and electrical transfer subsystem. This result applies to all orbit missions herein investigated.

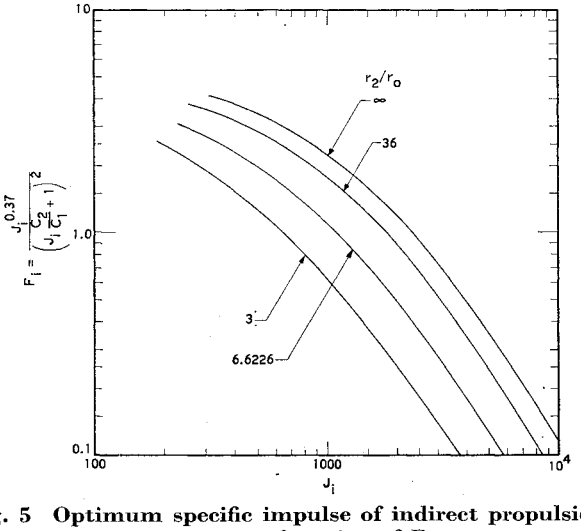

Fig. 5 Optimum specific impulse of indirect propulsion system as a function of F_i

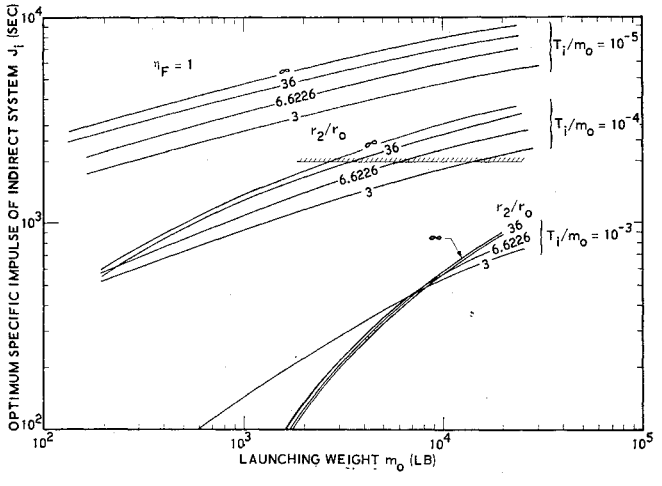

Fig. 6 Optimum specific impulse of direct propulsion system as a function of m_0, T_i/m_0, and r_2/r_0

For the thrust to weight ratio $T_i/m_0 \leqq 10^{-4}$, the optimum specific impulse of the indirect system is higher than the maximum specific impulse of the direct system provided the initial mass is greater than $m_0 \geqq 10^3$ lb at $r_2/r_0 = 3$ and $m_0 \geqq 500$ lb at $r_2/r_0 \to \infty$. For $T_i/m_0 = 10^{-5}$, the optimum specific impulse $(J_i)_{opt}$ is always larger than the maximum specific impulse of the direct system. Figure 6 also indicates that for $T_0/m_0 = 10^{-5}$ the high specific impulses required can be achieved only by advanced plasma accelerators, combined arc-jet-MHD accelerators, or ion engines, whereas for $T_0/m_0 = 10^{-4}$ the arc jet appears feasible with $J = 2000$ sec[10], or initial masses up to $m_0 = 1.5\cdot10^4$ lb at $r_2/r_0 = 3$ and $m_0 = 2.4\cdot10^3$ lb at $r_2/r_0 \to \infty$. Above these initial mass limits, arc-jet-MHD accelerators or ion engines are necessary to achieve the required optimum performance.

From a practical engineering point of view, extremely slow missions characterized by $T_0/m_0 \leqq 10^{-5}$ may be considered only for special, scientific, or academic experiments. For the medium time transfer missions with $T_i/m_0 = 10^{-4}$, the potential of arc-jet-MHD acceleration is very promising,[11] but the weight penalty of the necessary high field strength magnets and the complexity of present laboratory assemblies make immediate applications doubtful. Therefore, it is also necessary to investigate the performance of the indirect system for pure arc jet propulsion methods with specific impulse limitations of $J_i = 1200$, 1600, and 2000 sec. The latter value may appear somewhat optimistic at present but should be achievable in the near future, especially when schemes as those proposed by Ref. 12 are developed and refined to flight hardware. For specific impulse limited indirect propulsion systems, the payload ratio may be determined conveniently by assuming $(m_w/m_0)_i$ and γ_i to be independent for the first approximation. Then Eq. (3) determines the payload ratio of the specific impulse limited system, which is identified by an asterisk in this report:

$$\left(\frac{m_p}{m_0}\right)_i^* = \left(1 - \frac{1}{(C_3/C_4)J_i^* + 1}\right)^2 - k_s \quad (33)$$

where

$$\gamma_i^* = \left(\frac{1}{(C_3/C_4)J_i^* + 1}\right)^2 \quad (34)$$

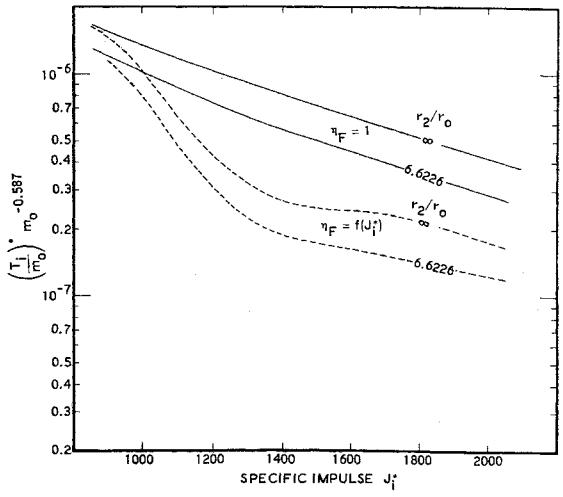

Fig. 7 Thrust to weight parameter of specific impulse limited indirect systems

The thrust to mass ratio $(T/m_0)^*$ corresponding to each solution of Eq. (33) is obtained by setting equal Eqs. (3) and (26) and by using Eq. (28) for the acceleration parameter:

$$\left(\frac{T_i^*}{m_0}\right) = \frac{J_i^{0.587} m_0^{0.587}}{\varphi_i C_4^{1.59}[C_3/C_4 J_i + 1]^{3.17}} \tag{35}$$

At this point it should be noted that $(T_i/m_0)^*$ is not an optimum value, but a "characteristic" value. It means the payload ratio $(m_p/m_0)_i^*$ corresponding to $(T_i/m_0)^*$ is decreasing for $(T/m_0)_i > (T/m_0)_i^*$ and is increasing for values of $(T/m_0)_i < (T/m_0)_i^*$ [Eq. (29)]. Figure 7 presents the characteristic thrust to mass ratio parameter θ, defined by

$$\theta_i = (T_i/m_0)^* \cdot m_0^{-0.587} \tag{36}$$

as a function of the specific impulse J_i^*, the frozen flow efficiency η_F, and the mission parameters $r_2/r_0 = 6.6226$ (synchronous orbit) and $r_2/r_0 \to \infty$ (escape). Figure 7 indicates that $(T_i/m_0)^*$ is decreasing with increasing values of J_i^* and the frozen flow efficiency η_F corresponding to each specific impulse. For r_2/r_0 and m_0 increasing, the thrust to weight ratio (T_i^*/m_0) is also increasing, indicating faster missions for increased initial masses. Figure 8 presents the characteristic thrust to weight ratio $(T/m_0)_i^*$ as a function of the initial weight, the specific impulse J_i^*, and the mission parameter $r_2/r_0 = 6.6226$. Figure 8 illustrates that for decreasing initial masses m_0 the thrust to weight ratio should decrease in order to achieve a constant payload ratio [Eq. (33)] for a given, constant value of J_i^*. The ratio $(T/m_0)_i^*$ also is decreasing with increasing values of J_i^* and with the frozen flow efficiency η_{Fi}.

Comparison of Indirect and Direct Systems

By use of the payload ratios derived for the direct and indirect system, the payload efficiency defined by Eq. (5) can be calculated and the performance of each method can be compared for a prescribed mission (r_2/r_0), initial mass m_0, and transfer time $\Delta t \sim (T_i/m_0)^{-1}$. For example, values of the payload efficiency greater than unity, $\eta_p > 1$, indicate that the indirect system is more efficient, whereas for $\eta_p < 1$ the direct system is superior. Figure 9 summarizes the performance of direct and indirect solar propulsion systems for the following conditions:

1) Thrust to weight ratio: $T_i/m_0 = T_0/m_0 = 10^{-4}$
   a) Transfer time: $\Delta t_i = \Delta t_0$
   b) Mission parameter: $3 \leqq r_2/r_0 \leqq \infty$
2) Frozen flow efficiency: $\eta_{Fi} = 1$ $\quad \eta_{Fi} = f(J_i)$
3) Specific impulse of direct system: $J_0 = 900$ sec

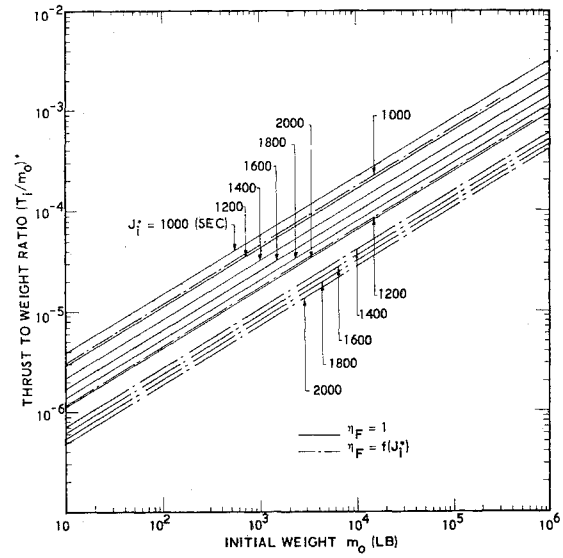

Fig. 8 Characteristic thrust to weight ratio $(T_i/m_0)^*$ of impulse limited indirect systems

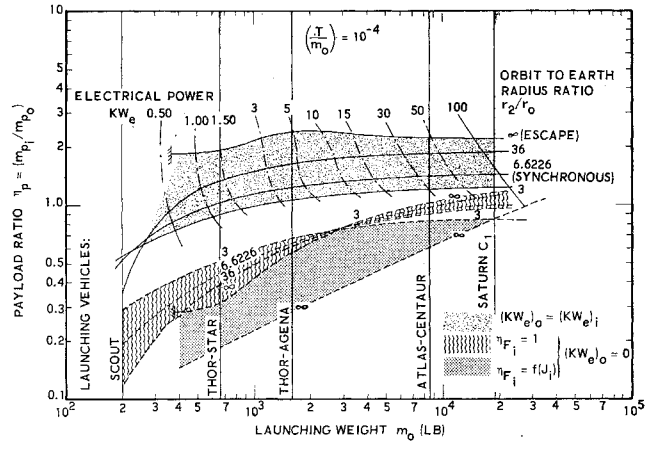

Fig. 9 Performance comparison of optimized indirect and direct solar propulsion systems

4) Specific impulse of indirect system: $(J_i)_{opt}$
5) Initial mass: $200 \leqq m_0 \leqq 2 \cdot 10^4$ lb
6) Structural mass ratio: $k_s = 0.10$

The curves, identified with $(kw_e)_0 = 0$ and $\eta_{Fi} = 1$, illustrate the performance of the indirect and direct system whereby equilibrium propellant flow has been assumed for the indirect system, and the direct system does not carry any additional power supply on board. The $(kw_e)_0 = 0$, $\eta_{Fi} = f(J_i)$ curves compare the indirect system and the direct system without additional power but include the effect of frozen flow efficiency upon the performance of the indirect system. The shaded curves labeled $(kw_e)_0 = (kw_e)_i$ represent the payload efficiencies for the condition that the direct system carries along a thermally integrated power supply subsystem that is capable of the same electrical power output as the powerplant of the indirect system operating with $\eta_{Fi} = 1$ and $\eta_{Fi} = f(J_i)$. The electrical power is intended for operation of the payload equipment in orbit. In view of Figure 9 and previous discussions, the following performance range is indicated for each propulsion system:

1) For propulsion purposes only the direct system is more efficient than the indirect system up to initial masses of $m_0 \leqq 1.5 \cdot 10^4$ for $\eta_{Fi} = 1$, whereas for frozen flow conditions the direct system out-performs the indirect system for all sole propulsion missions investigated and possible with present boost vehicles including the Saturn C_1.

2) For missions that require electrical power equal to or more than the electrical power output necessary for indirect

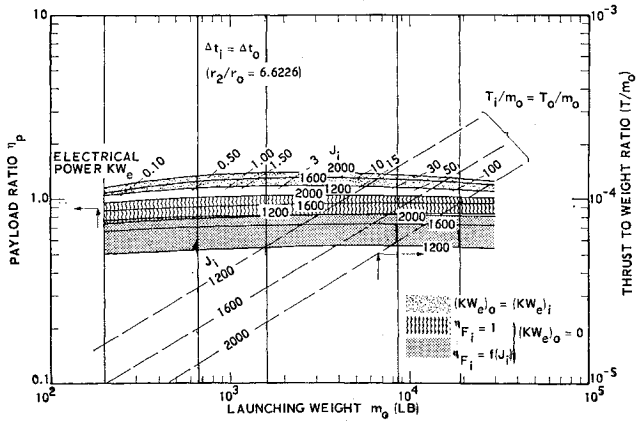

Fig. 10 Performance comparison of specific impulse limited indirect and maximum specific impulse direct systems for $r_2/r_0 = 6.6226$

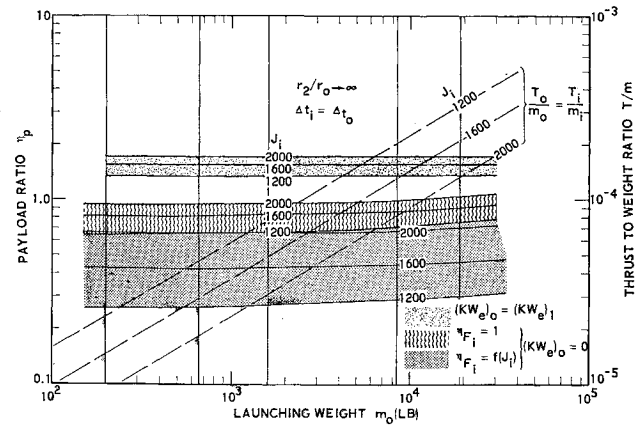

Fig. 11 Performance comparison of specific impulse limited indirect and maximum specific impulse direct systems for $r_2/r_0 \to \infty$

propulsion, the indirect system is more efficient than the direct system for initial masses $m_0 > 600$ lb. The electrical power as shown by the superimposed curves in Fig. 9 ranges from 1 kw to 100 kw for $600 \leqq m_0 \leqq 2 \cdot 10^4$ lb of initial mass.

3) For initial masses $m_0 \leqq 8.5 \cdot 10^3$, Fig. 9 indicates that the direct system could operate efficiently as a hybrid system, which should be of interest for all missions requiring additional but relatively small power supplies as payload.

4) The mission parameter r_2/r_0 has little effect on the performance of the direct system, specifying sole propulsion, whereas the performance of the indirect-power-on-board-system increases greatly with increasing values of r_2/r_0.

5) The performance of high powered indirect systems can be achieved only when large scale, accurate, solar collectors have been developed and the performance of present arc jets and arc-jet-MHD accelerators have been improved. Otherwise, the direct system and the hybrid system are the only promising solar propulsion methods for orbit missions.

6) For missions identified by thrust to mass ratios, $T_0/m_0 > 10^{-4}$, the performance of the direct and hybrid system increases since the optimum specific impulse of the indirect system decreases and the additional fuel weight and powerplant weight cannot be compensated during fast missions as discussed previously. However, for long transfer time missions, $T_i/m_0 \leqq 10^{-4}$, the performance of the indirect system becomes more efficient than that of the direct system; this is due to the increased fuel saving of the indirect system operating at higher specific impulses than the direct propulsion system.

For the case of specific impulse limited indirect propulsion, Figs. 10 and 11 present the payload efficiency η_p for the mission parameters $r_1/r_0 = 6.6226$ and $r_2/r_0 \to \infty$, and similar conditions as those listed previously. The following conclusions may be drawn when inspecting both diagrams calculated for $\Delta t_i = \Delta t_0$, but $T/m_0 \pm$ const.

1) For sole propulsion purposes the direct and indirect systems are about equal, provided equilibrium propellant flow can be achieved. In the case of frozen flow conditions, the direct system is unquestionably superior.

2) The thrust to weight ratio $(T/m_0)_i{}^*$ has to be decreased with decreasing values of the initial mass, m_0, and increasing values of the specific impulse $J_i{}^*$ in order to achieve the performance presented by Figures 10 and 11. This means that small launching masses require extremely long transfer times in order to reach payload ratios achievable by high initial mass systems with short transfer times.

3) For powered-payload missions, the performance of the indirect system is superior as shown previously and increases with increasing values of the mission parameter, r_2/r_0. For missions less than $r_2/r_0 \leqq 6.6226$, it is indicated that, for specific impulse limited indirect propulsion, there is little difference between direct and indirect payload capability. In this case it will be more practical to use the direct and/or the hybrid system, which promise a higher degree of reliability due to the basic simplicity inherent in these systems.

Finally, it is interesting to compare the performance of the hybrid communication satellite[2] and the performance of the French "Phaeton" indirect propulsion system[10] with the performance predicted by Figs. 9–11. Reference 2 proposed to transfer a communication satellite of initial weight $m_0 = 8170$ lb from a low-altitude orbit to the synchronous orbit $r_2/r_0 = 6.6226$ by means of a direct solar propulsion system. For operation of the communication equipment, Ref. 2 estimated that 5 kw of electrical power would be sufficient for presently planned systems. For this purpose Ref. 2 suggested a thermally integrated hybrid system because of early availability and simplicity of design. Inspection of Fig. 9 for optimum specific impulse and of Fig. 10 for specific impulse limited indirect propulsion systems indicates that if equilibrium propellant flow cannot be achieved (not likely in the near future) the choice of the hybrid system using direct propulsion is optimum for the considered mission. This is in excellent agreement with the detailed design study of Ref. 2.

The French Phaeton-satellite design has been described briefly in Ref. 10. There it is reported that the French organization SEPR (La Société d'Etude de la Propulsion par Réaction) is developing a highly efficient, 2.25 kw_e solar mechanical powerplant that will provide electrical power for indirect propulsion and operation of the payload instruments. Based on the high efficiency of this powerplant, the indirect propelled satellite Phaeton weighs only 600 lb and is scheduled for low-orbit and synchronous orbit missions. Figure 9 indicates that indirect propulsion is the optimum propulsion method for the power on board missions, provided that the missions start at an initial low orbit of 400 naut miles, the thrust-to-weight ratio is selected equal to or less than $T_i/m_0 \leqq 10^{-4}$, and low-orbit missions, identified by $r_2/r_0 < 4$, are avoided. However, in case the 2.25 kw_e, electrical power is not fully used for operation of the payload equipment, Figs. 9 and 10 show clearly that the direct or hybrid propulsion methods are superior. Figure 9 also indicates that Phaeton could be launched by a Thor-Star booster and that according to advanced United States concepts a 1 kw_e to 1.5 kw_e powerplant should be sufficient for executing the missions of interest.

References

[1] Carver, G. P., Linhardt, H. D., et al., "Feasibility investigation of solar rocket propulsion," Aeronutronic/Research Lab. Publ. no. P-12421 (U) (January 1962).

[2] Macauley, B. T., "Integrated low thrust solar propulsion-power generation system for communication satellites," Soc.

Automotive Engrs. Paper 346 B (1961).

[3] Linhardt, H. D., Carver, G. P., et al., "Long endurance, electromechanical, solar powered satellite powerplant," Aeronutronic/Research Lab. Publ. no. P-10722 (C) (1962).

[4] Irving, T. H. and Blum, E. K., "Comparative performance of ballistic and low-thrust vehicles for flight to mars," *Vistas in Astronautics* (Pergamon Press, New York, 1959), Vol. II, p. 202.

[5] Melbourne, W. G., "Interplanetary trajectories and payload capabilities of advanced propulsion vehicles," Jet Propulsion Lab., Pasadena, Calif., TR 32-68 (March 1961).

[6] Sanborn, D. S., "The development of deployable solar concentrators for space power," Ryan Aerospace, San Diego, Calif. (1961).

[7] Jack, J. R., "Theoretical performance of propellants suitable for electro-thermal jet engines," NASA TN D-682 (March 1961).

[8] Rudy, J. A., Liechty, D. W., and Taylor, T. E., "A preliminary installation study for project sunflower," *Propulsion, Space Science and Space Exploration* (Academic Press, New York, 1961), p. 39.

[9] Macauley, B. T., "Development of a high powered solar mechanical engine," Sundstrand Aviation, Denver, Colo. (1961).

[10] Poirer, B., "Phaeton—most advanced French design," Missiles and Rockets **10**, no. 19, 41–42 (May 7, 1962).

[11] Russell, G., "Development of an arc-jet-MHD accelerator," Aeronutronic/Research Lab., Internal Rept. (July 1962).

[12] Noeske, H. O. and Kassner, R. R., "Analytical investigation of a bi-propellant arc-jet," ARS Preprint 2125-61 (October 1961).

JULY 1963 AIAA JOURNAL VOL. 1, NO. 7

Orientation of Spinning Satellites by Radiation Pressure

Louis A. Ule*
Hoffman Electronics Corporation, Los Angeles, Calif.

By means of an array of mirrors or other optical devices, the force of radiation pressure is used to orient the spin axis of an artificial earth or sun satellite to the sun. The array also may produce spin-up or despin torques, be free of such torques, or regulate the spin rate to a predetermined value. This method of orientation, being stable, passive, and heliotropic, is particularly advantageous for small artificial satellites that derive their electrical power from solar cells.

Nomenclature

A = area of plane surface intercepting radiation
A_s = area of spin regulating surface
F_a = force parallel to spin axis
F_N = force normal to surface
F_s = force perpendicular to spin axis
F_T = force tangent to surface
i = angle of incidence of radiation from normal to surface
I = major principal moment of inertia
p_s = solar-radiation pressure
R = mean distance of a surface from the spin axis
R_i = inner radius of annular array
R_o = outer radius of annular array
R_s = mean distance of spin regulating surface from the spin axis
t = time, sec
T = torque
T_p = torque perpendicular to spin axis
T_s = despin torque
α = angle between reflector surface and spin axis
ϕ = angle about spin axis
θ = tracking error angle between angular momentum vector and radiation vector
ω = spin rate, rad/sec

Introduction

THE use of solar-radiation pressure for attitude control of an artificial satellite that will be described differs from previous methods in that it can be used only for a spinning vehicle. Methods of orientation by solar-radiation pressure suitable for nonspinning vehicles have been described by Sohn,[1] Frye and Stearns,[2] Newton,[3] and Villers and Olha.[4]

Received by ARS October 12, 1962; revision received May 16, 1963.

* Senior Staff Engineer, Military Products Division, Space Power Systems.

The method consists of an array of mirrors or other optical devices on the spinning satellite, arranged to acquire angular momentum from radiation pressure that will make the spin axis precess to the source of radiation.

Required Attitude Control Torque

To be continually directed to the sun, the spin axis of an earth satellite must be precessed at the rate of only 2×10^{-7} rad/sec. Accordingly, the torque required for precession, being very small, is compatible with the forces available from radiation pressure. An earth satellite with a major principal moment of inertia of 10 kg m^2 turning at 1 rpm would require only 0.02 dyne-m of torque to be developed from a solar-radiation pressure of about 1 dyne/m^2.

Mechanisms for Producing Precession Torques from Radiation Pressure

Radiation pressure cannot be made to produce a pure torque; however, forces due to light pressure on a rigid body can be produced such that in addition to a net push, there will be unbalanced forces about the center of inertia. Such torques have been the means proposed for orienting nonspinning satellites.[1–4]

The design of devices to produce a torque of fixed direction on a spinning satellite is somewhat more involved. The forces on different parts of the satellite cannot be made to differ simply, as any net effect on angular momentum in 1 revolution would be zero. Rather, the force of light pressure should be made dependent on the angle of incidence on a particular surface element in such a manner that, as the satellite spins, angular momentum is accumulated.

The torque that is required is not such as to spin-up or despin the satellite but is in a direction perpendicular to the